ORIGINAL PAPER

On radiative forcing of sulphate aerosol produced from ion-promoted nucleation mechanisms in an atmospheric global model

Hashmi Fatima · H. C. Upadhyaya ·
S. N. Tripathi · O. P. Sharma · Fangqun Yu

Abstract A significant fraction of the total number of particles present in the atmosphere is formed by nucleation in the gas phase. Nucleation and the subsequent growth process influence both number concentration of particles and their size distribution besides chemical and optical properties of atmospheric aerosols. Sulphate aerosol nucleation mechanisms promoted by ions have been evaluated here in a tropospheric interactive chemistry-aerosol module for mass and number concentration in a global atmospheric model. The indirect radiative forcing of sulphate particles is assessed in this model; indirect radiative forcing is different for ion-induced (IIN) and ion-mediated (IMN) mechanisms. The indirect radiative forcing in 10-year simulation runs has been calculated as -1.42 W/m^2 (IIN) and -1.54 W/m^2 (IMN). The 5% emission of primary sulphate particles in simulations changes the indirect radiative forcing from -1.42 to -1.44 W/m^2 for IIN case, and from -1.54 to -1.55 W/m^2 for the IMN case. More precisely, owing to greater nucleation rates, IMN mechanisms produces greater cooling than the IIN mechanisms in the backdrop that both mechanisms produce almost identical distribution of CDNC in their pre-industrial runs. The inclusion of primary particles in simulations with IIN and IMN mechanisms increases both CDNC and the indirect radiative forcing.

H. Fatima (✉) · H. C. Upadhyaya · O. P. Sharma
Centre for Atmospheric Sciences,
Indian Institute of Technology, Delhi, India
e-mail: hashmifatima@gmail.com

S. N. Tripathi
Department of Civil Engineering,
Indian Institute of Technology, Kanpur, India

F. Yu
Atmospheric Sciences Research Centre,
State University of New York, 251,
Fuller Road, Albany, NY 12203, USA

1 Introduction

Knowledge of new particle formation in the atmosphere is necessary because significant fraction of such particles act as cloud condensation nuclei (CCN) to produce several indirect effects among which the first effect is known after Twomey (1959, 1977). The ability for new particles to grow to CCN size depends on the pre-existing size distribution of particles and the condensational growth rate of new particles (Pierce and Adams 2009). It has been proposed that in many atmospheric regimes, nucleation and subsequent growth of fresh particles is the dominant pathway for the formation of CCN (Pirjola et al. 2002; Laaksonen et al. 2005; Spracklen et al. 2008; Wang et al. 2009; Yu and Luo 2009). Therefore, nucleation is one of the highly investigated topics towards understanding its influence on CCN. Boundary layer nucleation (BLN) from cluster activation theory to particle number in a global model was studied by Spracklen et al. (2006) and found that particle concentrations in remote continental regions were likely dominated by nucleated particles in contrast to polluted continental regions that were likely dominated by primary particles. Further, Spracklen et al. (2008) expanded this work to examine the impact of BLN events on CCN in the boundary layer and to explore the effect of uncertain secondary organic aerosol (SOA) condensation rates on the relationship between nucleation and CCN. However, a recent study (Metzger et al. 2010) provides the evidence for the role of organics in the aerosol particle

formation under atmospheric conditions, and suggests that particle formation is proportional to the product of concentrations of an organic molecule and sulphuric acid. This mechanism of new particle formation when parameterized in a global aerosol model substantially improved the simulations to agree with ambient observations on particle concentrations. Similarly, Makkonen et al. (2009) explored the sensitivity of aerosol and cloud droplet number concentrations to boundary layer nucleation rates and SOA formation rates. Particles formed by nucleation, grow to measurable sizes with sufficient sun exposure and relatively low preexisting aerosol surface area, which affect cloud droplet formation and radiative fluxes (Lee et al. 2003). A recent work of Wang and Penner (2009) emphasized the importance of nucleation and the inclusion of primary sulphate particles for CCN concentrations and their influence on aerosol indirect forcing. Although the chemistry transport models are quite in vogue, yet an atmospheric general circulation model (AGCM) coupled with interactive chemistry and aerosol processes may offer some advantages. Therefore, we use an interactive chemistry and aerosol module in an AGCM, so that chemistry and aerosol fields evolve consistently with the simulated meteorology in the global model.

Neutral binary nucleation of gaseous sulphuric acid and water vapour is no longer believed to be a major mechanism in the formation of atmospheric aerosols, especially in the lower troposphere (Weber et al. 1996; Clarke et al. 1998; Yu and Luo 2009; Yu et al. 2010). Alternative pathways for sulphate aerosol formation are therefore suggested in the literature. Chang et al. (2009) compared various mechanisms in CMAQ model, such as the neutral ternary nucleation (water–sulphuric acid–ammonia), ion-induced nucleation (IIN) of water and sulphuric acid with an empirical formulation. Lucas and Akimoto (2006) analysed binary, ternary and ion-induced nucleation mechanism in a 3D chemical transport model and found that ternary nucleation rates are unrealistically high in troposphere and IIN rates are negligible in the lower troposphere. Yu et al. (2008) showed that ion-mediated nucleation (IMN) could lead to significant new particle production in the entire troposphere. More recently, IMN has been shown to be able to account for both absolute values (within about a factor of 2) and spatial distributions of particle number concentrations observed in different parts of troposphere via land-, ship-, and aircraft-based measurements (Yu and Luo 2009). Though various mechanisms of nucleation have been studied, it is not yet clear what percent of particles in the aerosol population has been contributed by an individual mechanism in the atmosphere. But once the particles have formed and are allowed to grow, one can study their impact on climate in a global model with interactive chemistry and aerosol processes. On this premise, model

simulations with different nucleation mechanisms would then permit their comparison from the response they produce in radiative forcing. Moreover, an individual nucleation mechanism can very easily be examined and evaluated in a global model, if not in the atmosphere.

This study compares two ion-facilitated mechanisms for the first time by analyzing the radiative forcing they produce in an AGCM. Ion-facilitated nucleation mechanisms could be important in the upper troposphere, over oceans or even the entire globe. A comparative evaluation of particle formation by IIN and IMN mechanisms does require setting of appropriate ranges of meteorological variables and sulphuric acid vapour concentration in a global model because their validity ranges are different but overlapping. Numerical simulations have been performed by individually switching them on, one at a time in the AGCM. The ion-induced nucleation (IIN) mechanism is the parameterization of Modgil et al. (2005), which is based on the thermodynamic model of Lovejoy et al. (2004); while the ion-mediated nucleation (IMN) as ported in the model, is developed by Yu and colleagues (Yu and Turco 2000; Yu 2006; Yu and Luo 2009). Though the role of organics in the formation of new particles in the atmosphere has been emphasized by Metzger et al. (2010), SOA has not been parameterized in the aerosol module yet, hence the results of this study should be interpreted in the light of this important omission.

Although a more comprehensive comparison of various nucleation mechanisms has been presented in a recent study by Yu et al. (2010), which also includes a comparison of IIN and IMN mechanisms among others, this study lays emphasis on indirect radiative forcing arising from new particles forming due to nucleation. A notable contribution on the indirect forcing of nucleated particles is a recent study by Wang and Penner (2009), which suggests that indirect radiative forcing largely depends on relative changes of primary emitted particles and SO_2 emissions from the preindustrial levels. It is possible to make an estimate of the indirect aerosol forcing within the framework of interactive chemistry and aerosol dynamics in a global model, because fresh particles after growth and coagulation could turn into cloud condensation nuclei leading to cloud formation in atmospheric moist regions. Indeed, high aerosol number concentrations are responsible for non-precipitating closed-cell reflective clouds, whereas low aerosol concentrations favour open-cell precipitating clouds and to produce oscillation in open cellular cloud patterns (Feingold et al. 2010).

It is apparent from the above discussion that the possibility of ion-facilitated nucleation occurring in the atmosphere could be important though some controversy exist in respect of IMN (Yu 2010). However, the aim of this study is to compare the ion-induced nucleation (IIN)

mechanism (Modgil et al. 2005, Lovejoy et al. 2004) and the ion-mediated nucleation (IMN) mechanism (Yu and Turco 2000; Yu 2006, Yu 2010, Yu et al. 2010) by appropriately setting the ranges for relevant parameters in a global model.

2 The model description

The global model used for this study is the standard general circulation model (Sadourny and Laval 1984) of Laboratoire de Météorologie Dynamique (LMDZ version 3.3) with interactive chemistry and aerosol dynamics as described in Verma et al. (2007). LMDZ is a grid point global climate model with a resolution of $3.75^°$ in longitude and $2.5^°$ in latitude. It has 19 vertical layers in hybrid sigma pressure coordinate, with 6 layers below 600 hPa and 9 layers above 250 hPa. The chemical species are advected in the model and evolve consistently with dynamical, physical, and chemical processes as model integration advances in time. The chemistry module includes anthropogenic and biogenic emissions; over 50 gas/aqueous phase chemical reactions (33 gas phase and 18 aqueous phase) along with the sources and sinks of chemical species that are considered in the model. The present model LMDZ.3.3 has chemistry up to troposphere only. The sulphuric acid vapour produced from gas phase chemistry drives the two-mode, two-moment aerosol module which calculates besides other parameters, the aerosol mass, number concentration and particle surface area for the Aitken and accumulation modes; while the sulphate from aqueous phase oxidation largely goes in the accumulation mode. This aerosol module has been adapted in LMDZ from Model-3/CMAQ of US Environmental Protection Agency (EPA), which has been described in detail by Binkowski and Roselle (2003).

The prognostic chemical species in the LMDZ model are water vapour, liquid water, dimethylsulphide (DMS), hydrogensulphide (H_2S), dimethylsulphoxide (DMSO), methanesulphonic acid (MSA), sulphur dioxide (SO_2), oxides of nitrogen (NOx), carbon monoxide (CO), ozone (O_3), hydrogen peroxide (H_2O_2), and sulphate aerosol mass and number for Aitken (0.005–0.1 μm) and accumulation modes (0.1–2.5 μm). Further, the gas phase chemistry also takes into account the cloud effects in calculating the photolytic rates. When clouds are present, the clear sky photolytic rates in this model are multiplied by a correction factor. In-cloud aqueous phase reactions are major contributors to atmospheric sulphate. In the present model, aqueous phase oxidation of SO_2 by O_3 and H_2O_2 are considered. The SO_2, H_2O_2 and O_3 concentrations in cloud droplets are assumed to be in equilibrium with the gas

phase concentration and are carried as implicit fields; that is, they are computed as a function of gas phase concentrations. The CO_2 concentration is held constant (370 ppm) throughout the model integrations. The aqueous phase chemistry is active only in the cloudy portion of the grid cells and in the presence of liquid water. The aqueous phase oxidation in ice clouds has not been considered. Both in-cloud and below-cloud scavenging has been included in the model. Thus, the model used in this study is fairly complete and comprehensive.

The performance of the LMDZ model coupled with chemistry and aerosol modules, has been thoroughly evaluated (Verma et al. 2007) by comparing observations with the simulated oxidants (mainly hydroxyl radicals and O_3), aerosol mass and number concentrations in a 24-month integration of the coupled system. From this evaluation, it has been found that the model overestimates ozone by about 10 ppbv at lower levels and within a factor of two in upper troposphere from observations at most of the sites. The model also simulated lower ozone concentrations over eastern China, which translated into underestimations of the simulated sulphate mass. It may be remarked that one-to-one agreement between observations (IMPROVE network over North America and EMEP over Europe) and simulated values at observation locations is very difficult because models simulate grid-averaged values of a prognostic parameter while observations are point values. Hence, the model used for this study was further evaluated for annual sulphur cycle; the sulphur budget values pertaining to turnover times and yields are consistent with other modelling studies. Thus, LMDZ with interactive tropospheric chemistry and aerosol modules as ported and described in Verma et al. (2007) appears to be a useful tool for studying other scientific problems of current interest related to sulphur chemistry and sulphate aerosols. Since the model specifies formation, transport, and deposition of sulphate aerosols, the direct and indirect forcing (Verma et al. 2006) could also be studies by prescribing aerosol optical properties, which depend on relative humidity.

2.1 The aerosol module

The gas phase chemistry provides the production rate of sulphuric acid vapour in the model, which drives the aerosol module. Since the gas- and aqueous phase chemistry are already described in Verma et al. (2007), their details have been omitted here; but, for the sake of clarity, we briefly describe the aerosol module wherein the IIN and IMN mechanisms of particle formation have been included to carry out this study. However, for fuller details on this state-of-the-art "modal" aerosol model, one may refer to

the papers of Binkowski and Shankar (1995) and Binkowski and Roselle (2003); its initial evaluation has been given by Mebust et al. (2003) with the observations of sulphate, nitrate, $PM_{2.5}$, PM_{10} and organic carbon, and most simulated values fall within a factor of two of the observations. It should therefore be possible to compare different nucleation mechanisms of sulphate aerosol formation in the LMDZ model.

As mentioned earlier, the sulphuric acid vapours drive the aerosol model, which essentially assumes a lognormal distribution for aerosol particles in the Aitken, accumulation, and coarse modes. The Aitken mode includes particles with diameter up 0.1 μm and the accumulation mode particles have diameters in the range 0.1–2.5 μm. The third mode considered in the model is the coarse mode (dust) particles with diameters superior to 2.5 μm, however, the coarse particles are not considered in this study because it pertains to a comparison of two ion-facilitated nucleation mechanisms. Another important omission is the inclusion of SOA in the model, though the SOA has been added in a recent version of aerosol model in CMAQ (Foley et al. 2010). However, the consideration of SOA could justifiably be omitted in this comparison study because the existing models notably underestimate (up to 90%) the mass concentration of SOA in the atmosphere (Herald et al. 2005; Makkonen et al. 2009). This omission would also preclude possible high level of uncertainty in the simulations with ion-facilitated mechanisms.

Since we consider only the Aitken and accumulation modes in this study, the prevalence of aerosol particles in the model is described by a bimodal lognormal distribution,

$$n\left(\ln d\right) = \frac{N}{\sqrt{2\pi}\sigma_g}\exp\left[-0.5\left(\frac{\ln\frac{d}{d_g}}{\ln\sigma_g}\right)^2\right] \qquad (1)$$

where N is the particle number concentration within the mode, d is the particle diameter, d_g and σ_g are the geometric mean diameter and geometric standard deviation of the modal distribution, respectively. The geometric standard deviation has been fixed as 1.6 for Aitken mode and 2.0 for the accumulation mode. Both intramodal and intermodal coagulation of particles is considered in the model. Further, particle growth takes place due to condensation of sulphuric acid vapours on the pre-existing particles. The smaller Aitken particles when grow to the size of accumulation mode during simulations, a mode merging algorithm, which considers the growth rate of the Aitken mode particles, is used that transfers number, surface area and mass concentration from Aitken mode to accumulation mode. The numerical solver of the governing modal equations has been described in Binkowski and Roselle (2003).

2.2 Nucleation mechanisms

The aerosol module of CMAQ, as incorporated in the LMDZ model, has two new particle formation mechanisms due to Kulmala et al. (1998) and Harrington and Kreidenweis (1998a, b). Both mechanisms consider that sulphuric acid vapours produce new particles in the atmosphere. These two mechanisms have not been used in this study; instead, two new modules IIN and IMN mechanisms have been included, as mentioned above, in LMDZ model which have been compared from the long-term AGCM simulations performed with same set of initial and boundary conditions. While both these mechanisms assume new particle formation from nucleation of sulphuric acid vapour on charged ions (produced in the atmosphere by galactic cosmic radiation), there are nevertheless some key differences in the data that are used in formulating IIN and IMN mechanisms. These differences are evident from the following brief descriptions of the IIN and IMN mechanisms.

Lovejoy et al. (2004) described a kinetic ion nucleation model (SAWNUC) for calculating the particle formation rate based on measured thermodynamics of small ion and neutral clusters. An accurate kinetic treatment of atmospheric nucleation was not possible earlier due to lack of thermodynamic data for the relevant clusters. Lovejoy et al. (2004), for the first time, measured the thermodynamics for the binding of H_2SO_4 and H_2O to cluster ions of the form $HSO_4^-(H_2SO_4)_x(H_2O)_y$ and $H^+(H_2SO_4)_m(H_2O)_n$ and connected the laboratory measured small cluster thermodynamics to the bulk liquid drop limit to yield thermodynamic predictions for all cluster sizes and compositions. The SAWNUC model treats the kinetics of growth and evaporation of neutral and ionic clusters explicitly. The ion-induced nucleation rate (J_{iin}) is defined as the rate of formation of stable neutral cluster (i.e., larger than the critical cluster) by recombination of ionic clusters. Based on SAWNUC output, Modgil et al. (2005) derived a five-dimensional parameterization of IIN which is valid for the temperature range (190, 300 K), RH (0.05, 0.95), H_2SO_4 concentration (105, 108/cm^3), first order loss of H_2SO_4 to particles (0.00009, 0.0245/s) and ion source rate (2, 50) ion pairs/cm^3/s. Parameterized formulas are obtained for the five variables: (1) particle nucleation rate (2) H_2SO_4 nucleation rate, (3) number of H_2SO_4 molecules in average nucleating cluster, (4) number of H_2O molecules in average nucleating cluster, and (5) radius of average nucleating cluster. The parameterization generally reproduces the modelled nucleation rate to within an order of magnitude over the whole range of atmospheric conditions, except when the nucleation rate is very low (<10 cm^3/s), which corresponds to a rate lesser than 0.1 particle/cm^3/day

and extreme conditions, e.g., very low or high values of temperature, relative humidity, H_2SO_4, etc. However, these ranges were modified in the present simulations with the AGCM as Modgil et al. (2005) parameterization produced unrealistically higher nucleation rates in comparison to SAWNUC predictions.

The ion-mediated nucleation (IMN) model has been formulated by Yu and Turco (2001) and in a series of subsequent papers using a kinetic model that explicitly resolves the interactions between ions, neutrals, and charged clusters in the presence of water vapour molecules and pre-existing particles. It considers the binary H_2SO_4–H_2O system, which depends on the following variables: H_2SO_4 concentration (5×10^5–5×10^8/cm^3), relative humidity (0.5–99.5%), temperature (190–302 K), ionization rate (1.5–60 ion pairs/cm^3/s) and local surface area density of pre-existing particles (1–1,000 μm^2/cm^3). This model was further expanded by Yu (2006) to design a second-generation ion-mediated nucleation model. Yu (2006) developed a set of differential equations of evolution type to predict different compositions and sizes of clusters (neutral, positively charged and negatively charged). The thermodynamic data for small ion clusters are derived from a modified Kelvin-Thomson equation (Yu 2005) to accurately represent the dipole-charge interactions. The IMN mechanism with new thermodynamic data and physical algorithms (Nadykto and Yu 2003; Yu 2005) has been incorporated in a global chemical transport (GEOS-Chem) model (Yu et al. 2008), which also treats explicitly evaporation of neutral and charged clusters. The simulation results of GEOS-Chem model (with prescribed meteorological fields therein) have been validated with land-, ship- and aircraft-based measurements on particle formation. Here, the IMN module (Yu 2010) in LMDZ uses meteorological parameters (wind, temperature, humidity and clouds) as simulated in the AGCM; and, the chemical species, cloud properties, aerosol mass and number concentration evolve consistently with the simulated meteorology in the model. The nucleation rates (J_{imn}) at model grid points are estimated from a five-dimensional look-up table, which essentially reduces the computational cost making it viable in an AGCM. The look-up table has been derived for a wide range of atmospheric conditions from a recent version of IMN model in which uncertainty has been reduced with the help of two independent measurements to constrain monomer hydration in the H_2SO_4–H_2O system and energetics of small neutral H_2SO_4–H_2O clusters (Yu 2007). Thus, the look-up table provides J_{imn} and the properties of clusters under different meteorological states. Undoubtedly, instead of using the full IMN model as described in Yu (2006), the look-up table based estimates of J_{imn} are computationally efficient for its ready use in an AGCM to address even the problem of climate and its change.

The nucleation rates from IIN and IMN mechanisms may differ by several orders of magnitude. The J_{imn} from IMN mechanism is generally higher than J_{iin}, but as temperature increases beyond 290 K (i.e. T > 290 K), and [H_2SO_4] decreases below 1×10^6/cm^3 (i.e. [H_2SO_4] $< 1 \times 10^6$/cm^3), J_{iin} increases unrealistically and therefore, care has been taken to fix a range where the parameterization of Modgil et al. (2005) agrees well with the model of Lovejoy et al. (2004). One may set the value of J_{iin} to zero outside this range to filter out such unrealistic, large values when the parameterization of Modgil et al. (2005) is used. However, it may be pointed out that nucleation rates are much smaller when [H_2SO_4] $< \sim 1 \times 10^6$/cm^3 and temperature exceeds 290 K even with the IMN mechanism (Yu et al. 2010). Since temperature and sulphuric acid vapour concentration are the key parameters that control the formation rate of new particles, fixing their range appears to be most appropriate for comparing these two mechanisms in an AGCM. Nucleation rates are also sensitive to RH if it decreases below 20%, but as the RH values increases above this value the sensitivity decreases. The above mentioned sensitivity of the IIN and IMN mechanisms to temperature, [H_2SO_4], and RH mainly arises from different thermodynamic data used to represent the neutral H_2SO_4–H_2O binary system, differences in the treatment of positive ions/clusters (the dynamics of positive ion clusters not actually treated in the model of Lovejoy et al. 2004), and different thermo-chemical data for ion clusters not directly investigated in the laboratory by Lovejoy et al. (2004); or for which alternative data exist (Yu, 2006). It should be emphasized that the current version of the IMN model (Yu 2006, 2007) incorporates not only the thermodynamic data for small ion clusters used by Lovejoy et al. (2004), but also a number of other thermodynamic data sources and physically based schemes.

The nucleated embryos from the two ion-facilitated nucleation mechanisms are less than 1.5 nm in diameter; however, the aerosol module assumes newly formed particles of 3.5 nm in diameter. Therefore, it is necessary to estimate the rate of formation of particles with diameter 3.5 nm in the model. For this purpose, we follow the work of Kerminen and Kulmala (2002), and accordingly, the nucleation rate (J) in the model has been formulated in terms of J_{nuc} (equal to J_{iin} or J_{imn}) as

$$J = J_{nuc} \exp\left\{\frac{\eta}{d} - \frac{\eta}{d_{nuc}}\right\}, \quad \eta < 1 \qquad (2)$$

where d_{nuc} is the initial diameter of nucleated particles from either mechanism and $d = 3.5$ nm; the parameter η has been assigned a constant value in the simulations. Wang and Penner (2009) have also used relation (2) to calculate the nucleation rate of 3-nm particles in the CAM3/IMPACT model. The particles (assumed to be

sulphuric acid) further grow from this size by a combination of coagulation and condensation processes, which are well represented in the two-mode, two-moment aerosol model described by Binkowski and Roselle (2003). It may be remarked that if relation (2) were not used in the calculations, then assuming the diameter $d = 3.5$ nm for nucleating particles would amount to a gross simplification. Once J has been computed by either mechanism, the production rate for particle number (cm^3/s) is computed as.

$$\frac{dN}{dt} = J \qquad (4)$$

and the particle mass (µg/cm^3/s) as

$$\frac{dM}{dt} = \frac{\pi}{6}\rho d^3 J \qquad (5)$$

where ρ is the density of the sulphuric acid particle at ambient relative humidity (Nair and Vohra 1975). A rigorous check is made here that the formation rate computed from (5) should not exceed the input sulphuric acid vapour production rate computed in the gas phase chemistry module during model simulations. The surface area of the new particles is also calculated from a prognostic equation, which involves the nucleation rate calculated by Eq. 2.

2.3 Cloud droplet number concentration and optical properties

Coagulation (main sink of nuclei particles) and growth then turn the smaller particles into accumulation mode particles through three modes of condensation: growth due to condensation on existing particles, intramodal and intermodal coagulation; finally such grown up particles serve as cloud condensation nuclei in the model to calculate cloud droplet number concentration (CDNC) from the formulation of Jones et al. (1994). The sulphate number concentration is empirically related to CDNC (represented by N_d) as,

$$N_d = \text{MAX}\left[375\left\{1 - \exp\left(-2.5 \times 10^{-9} N_j\right)\right\}, N_{min}\right] \qquad (6)$$

where N_j is the sulphate aerosol number concentration in the accumulation mode and N_{min} has been set to a value 5 droplets/cm^3. From the number of cloud droplets (N_d) and the cloud water content (LWC), the cloud droplet effective radius can be calculated as (Martin et al. 1994)

$$r_e = \left(\frac{3\text{LWC}}{4\pi\rho_w\kappa N_d}\right)^{1/3} \qquad (7)$$

where ρ_w is the liquid water density and κ is the cube of the ratio of the mean volume radius and the effective radius of the cloud droplet spectrum. The parameter κ takes a constant value depending on whether the airmass is continental ($\kappa = 0.67$) or maritime ($\kappa = 0.80$). Using the integrated liquid water content (LWC) of a model layer, which

increases linearly with height z above cloud base, the liquid water path (W) of the layer is computed in the model as

$$W = \int_{z=0}^{h} \text{LWC} \times dz \qquad (8)$$

where h is the cloud thickness. From liquid water path, the cloud optical properties are determined which are used in the shortwave and longwave transfer calculations. For longwave computations (Morcrette 1999), the cloud emissivity (ε_c) is determined as

$$\varepsilon_c = 1 - \exp\{-aW\} \qquad (9)$$

where the absorption coefficient is taken as $a = 0.13$ for all cloud types. For shortwave calculations, the cloud optical thickness, an asymmetry factor, and a single scattering albedo of clouds are required. The asymmetry factor is set equal to 0.86 and 0.91 for the two shortwave bands 0.2–0.68 µm and 0.68–4.0 µm, respectively. The cloud optical thickness in the model is defined in accordance to the Mie theory (Fouquart and Bonnel 1980) as

$$\tau_c = \frac{3}{2}\frac{W}{\rho_w r_e} \qquad (10)$$

The model further accounts for the diurnal cycle of solar radiation. The shortwave radiative fluxes at TOA and at the surface are computed every 2-h with or without the presence of clouds and aerosols.

To model the radiative effects of aerosols, the spectrally resolved optical properties of sulphate aerosol are necessary. The optical properties of sulphate aerosol are obtained from Mie theory using a size distribution and measured data on the refractive index of aerosols (Tang and Munkelwitz 1994). These properties are computed at 24 wavelengths covering the entire solar spectrum (0.2–4 µm) and are then grouped into two model spectral bands (0.25–0.68 and 0.68–4 µm) as weighted averages with a typical spectral distribution of the incoming solar radiation flux at the surface. The average quantities over these two spectral bands also include variations arising with relative humidity (Boucher and Anderson 1995). Typically, the physical and optical properties at 550 nm of the dry sulphate aerosol are as follows:

Aerosol type	ρ (g/cm^3)	r_0 (µm)	σ_g	α_e (m^2/g)	ω	g	Refractive index
Sulphate	1.769	0.0355	2.0	4.311	1.00	0.609	1.53–0.0i

Here ρ is density, r_0 is modal radius, σ_g is geometric standard deviation, α_e is mass extinction coefficient, ω is aerosol single scattering albedo, and g is asymmetry factor.

3 Simulation experiments

Atmospheric ions are produced mainly by galactic cosmic rays (GCRs) that are known to be the principal agents of ionization in the atmosphere above 1 km altitude (Fig. 1). The GCR-induced ionization rates in the model are specified as a function of the 11-year solar cycle, latitude and altitude. Ions are lost by recombination with ions of the opposite polarity, and by attachment with aerosols. Moreover, the impact of GCRs over CCN is thought to be small (less than 0.1% between solar maxima and minima), but it is nevertheless important in cloud physics (Pierce and Adams 2009) because ion pair production rate ultimately limits the maximum nucleation rates for ion-induced and ion-mediated nucleation mechanisms. Since part of sulphuric acid vapour produced in gas phase chemistry first condenses on to existing particles in the aerosol module, the remaining part nucleates to produce new particles in the model. Thus, nucleation is an important component of the aerosol dynamics. When particle grow sufficiently in size, they could act as CCNs or could scatter radiation to effectively change the response of the model which could be assessed from radiative forcing. Thus, numerical simulations performed with an AGCM, which use the same set of initial, and boundary conditions could provide a reliable means of comparing different nucleation mechanisms on the basis of differences in the radiative forcing. Here,

numerical simulations have been performed with LMDZ.3.3 model at $96 \times 72 \times 19$ resolution. In all, four numerical simulations have been carried out with the model; and each simulation has been accomplished by performing a 10-year model run with prescribed initial conditions prepared from the 12 GMT ECMWF Analysis of 20.12.1997 and boundary conditions. The 10-year runs are required because the noise reduces in the simulated fields from such long-term simulations. The first year of the each simulation run is the spin-up period of the model, and results are analysed for the last 9-year period of the model run. The sea-surface temperatures provide important boundary forcing in the simulations and have been prescribed from the daily NCEP optimally interpolated SST data (ftp://eclipse.ncdc.noaa.gov/pub/OI-daily/NetCDF), while the surface albedo and sea-ice have been prescribed from climatology.

There is also a need for the emissions to be prescribed in numerical simulations. Hence, sulphur emissions from fossil fuel combustion and industrial processes are from GEIA (Global Emission Inventory Activity) for the base year 1985 (http://www.geiacenter.org). The range of input parameters for the IIN and IMN mechanisms is somewhat different, which necessitates setting up of common ranges for the input variables in this comparison study. The selection of common range is imperative, because IIN parameterization produced unrealistically higher nucleation

Fig. 1 Annual averages: zonal distribution of the input variables
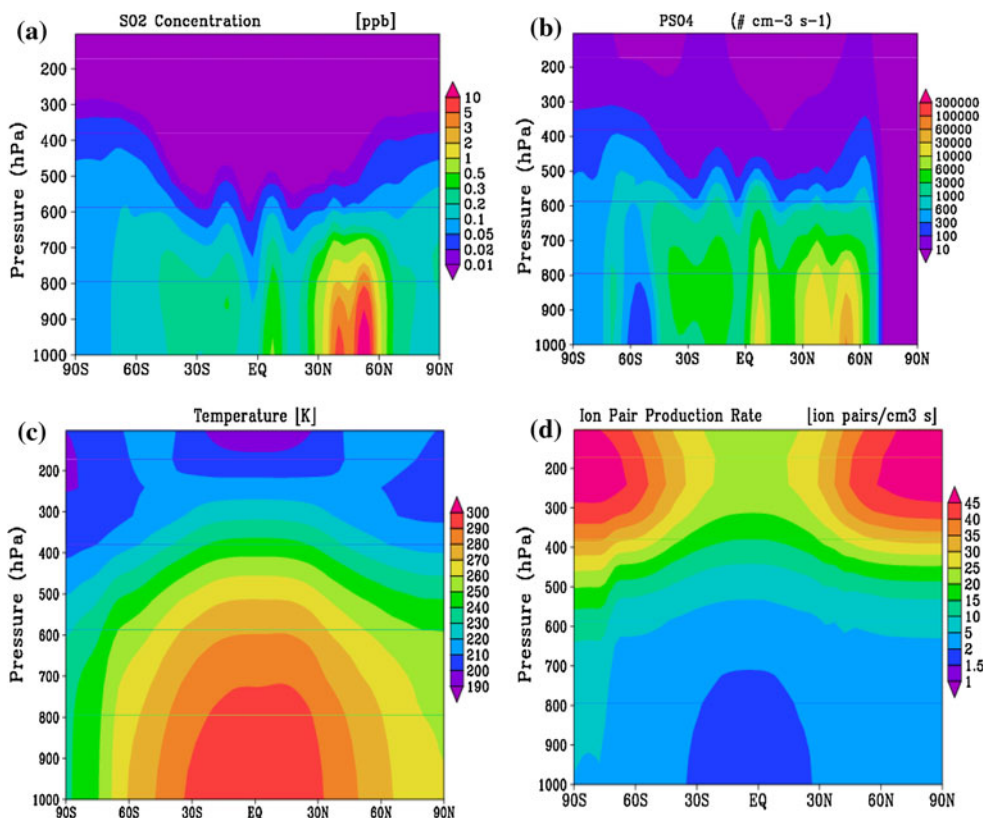
rates in comparison to SAWNUC predictions. Hence, the common range of input variables for both IMN and IIN parameterizations is: temperature (190–280 K), relative humidity (<0.95) ionization rate (2–50 ionpairs/cm^3/s) and pre-existing surface area (1–100 μm^2/cm^3). The lower limit for H$_2$SO$_4$ concentration is 1×10^6/cm^3. We have limited the RH up to 95% in view of the limitation of IIN on this parameter. Indeed, the model also includes aqueous phase chemistry and when RH exceeds 80%, clouds form in the model grids. In the cloud fraction of the grid, the aqueous chemistry will operate and SO$_2$ will be oxidized by the O$_3$ and H$_2$O$_2$. However, fixing 95% as the upper limit for RH in the model is certainly not a requirement and it could be relaxed without much difficulty.

Since primary particles, emitted directly from combustion sources or through the interplay of mechanical processes over land and ocean are sufficiently large to act as CCNs (Wang and Penner 2009). Hence, inclusion of primary particles is more realistic, so direct particle emission considered here from SO$_2$ emissions acts as "proxy" for such particles in this study. The mass of such particles in our model is added to the accumulation mode particles and from accumulation number particle concentration, CDNC is calculated from the formulation (6) of Jones et al. (1994). Thus, sensitivity runs with direct 5% sulphur emission from sources as grown up particles, have also been carried out to evaluate how the primary particles influence the indirect radiative forcing in the model. The following numerical experiments have been performed for this study:

1. IIN preindustrial run: model simulation with emissions prescribed at preindustrial era
2. IMN preindustrial run: model simulation with emissions prescribed at preindustrial era
3. IIN run: model simulation with present-day emissions and IIN mechanism
4. IMN run: model simulation with present-day emissions and IMN mechanism

One set of above types of experiments is performed without primary particle emission and another set of simulations is carried out with 5% emission of sulphate mass that goes directly into the accumulation mode. The simulated fields from these numerical experiments have been used to calculate the radiative forcing. Direct radiative forcing (DRF) is computed as the difference between the increments of shortwave fluxes at the top of the atmosphere when the contribution of sulphate aerosol is included or excluded in simulations. Whereas the indirect radiative forcing (IRF) is calculated as the difference between the increments of cloud radiative forcing simulated by the model with prescribed present-day emissions and those at the preindustrial levels. Thus,

$$IRF = CRF_{present} - CRF_{preindustrial} \qquad (11)$$

where CRF is defined as the difference of radiative fluxes between whole sky and clear sky conditions:

$$CRF = F_{wholesky} - F_{clearsky} \qquad (12)$$

The indirect radiative forcing is induced by the changes in cloud droplet radii, cloud water content, and cloud fraction due to the increase in anthropogenic emissions relative to emission levels of the preindustrial era. For calculating the indirect radiative forcing, two pairs of model integrations were run in parallel, one using preindustrial (natural) sulphur emissions, and the other using present-day (natural plus anthropogenic) emissions, and the difference in net cloud radiative forcing between the two runs provides an estimate of the radiative impact of aerosols.

4 Results and discussion

The zonal averages of input variables (SO$_2$, H$_2$SO$_4$ vapour, temperature, ion pair production rate) have been plotted in Fig. 1, neglecting the initial 1-year spin-up period in 10-year simulation runs. Average fields are then produced from the output of such 10-year runs using their values at the lowest 14 model layers, as the model includes only the tropospheric chemistry. The higher SO$_2$ concentration zones in Fig. 1a are generally seen confined over source regions. The relatively low concentrations of SO$_2$ especially in the upper troposphere in tropics could be due to relatively weak SO$_2$ sources and probably high scavenging rates associated with convection and precipitation in these regions. The relatively high SO$_2$ concentration over Antarctica arises mainly from DMS emissions near the Antarctic coast. The extension of high SO$_2$ zone from surface up to 700 hPa around 30°S is associated with mountain uplifting of anthropogenic SO$_2$ emission in Chile and direct injection of SO$_2$ into mid-troposphere from the continuously active volcano Lascar in Chile (2,400 Mg–SO$_2$/day, 23.32°S, 67.44°W, elevation 5.6 km).

The concentration of H$_2$SO$_4$ vapour (P$_{SO4}$) is determined by its production rate (mainly controlled by [SO$_2$] and [OH]) and the loss rate (condensation sink). From Fig. 1b, one may notice that higher [H$_2$SO$_4$] are confined to areas of higher SO$_2$ concentration, higher annual irradiance flux, and low condensation sink (CS). However, [H$_2$SO$_4$] would be higher, in effect, only when conversion of SO$_2$ dominates the regions with noticeable CS. The vertical distribution of [H$_2$SO$_4$] generally shows decrease with altitude following the SO$_2$ vertical profile. The zonal distribution of temperatures simulated by the model is given in Fig. 1c. The striking resemblance of the zonal

Fig. 2 Annual mean: zonal average of sulphate aerosol nucleation rates (cm^3/s)
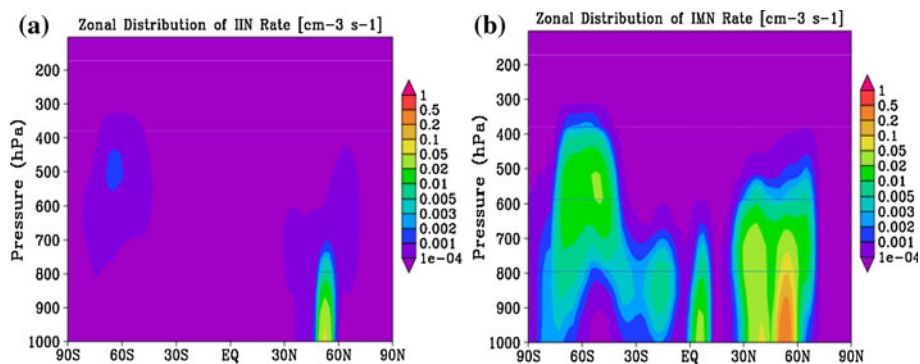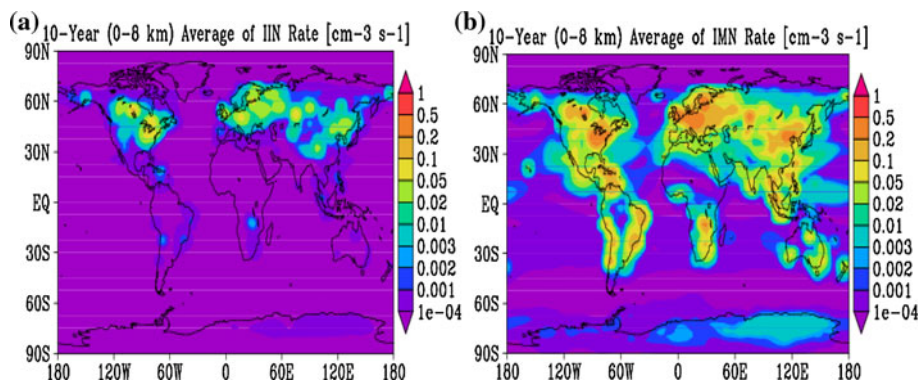

Fig. 3 Annual average: global distribution of sulphate aerosol nucleation rates (cm^3/s)

distribution of the ion pair production rate (Fig. 1d) from galactic cosmic rays to the zonal distribution of temperatures is notable but ion pair production rate is higher in the upper troposphere where temperatures are low. The low ion pair production rate in the boundary layer and the mid-troposphere is one of the main reasons that ion-induced nucleation is not efficient in the lower troposphere.

The zonally averaged distributions of nucleation rates from ion-facilitated mechanisms are shown in Fig. 2. Though the ion pair production rate is relatively low in the lower troposphere, but IMN mechanism simulates stronger nucleation rates in comparison to the IIN mechanism (Fig. 2a) throughout the troposphere. This result is consistent with the earlier findings (Yu et al. 2010, and references therein). The annual horizontal distribution of nucleation rates in the lower atmospheric layer (averaged in 8 km layer), are smaller by a factor of ∼5–10 for IIN than those simulated with IMN. Therefore, in the boundary layer IIN is less efficient in new particle formation than the IMN; a result that is expected. Accordingly, of the two mechanisms, the IMN mechanism would preferably work better in providing nucleation rates of particles in the boundary layer as well. Earlier, Spracklen et al. (2006) have emphasized the role of BLN in new particle formation. The horizontal distribution of simulated nucleation rates by two mechanisms (Fig. 3) in LMDZ.3.3 are quite similar to those presented by Yu et al. (2010) with GEOS-Chem model, despite the fact that chemistry in former is

just a subset of that in the latter. Nevertheless, the difference between this study and that of Yu et al. (2010) would naturally arise because GEOS-Chem model considers the most detailed chemistry of the atmosphere, whereas the LMDZ.3.3 chemistry considers only the dominant reactions of the tropospheric sulphate chemistry to obtain the sulphuric acid vapour production. Moreover, GEOS-Chem also includes an elaborate stratospheric chemistry and volcanic emissions, which are absent in the LMDZ.3.3 model. Another advanced feature of the GEOS-Chem model could be noted in the aerosol dynamics which employs 40 bins to size-resolve aerosol particles (Yu and Luo 2009, Yu et al. 2010), whereas in the present study a two-mode, two-moment aerosol model is employed to represent sulphate particles.

To analyse the indirect effects arising from nucleated particles, it is necessary to examine simulated CDNC with IIN and IMN mechanisms in the pre-industrial runs and the corresponding runs with present-day emissions. The zonally averaged cloud droplet number concentrations (CDNCs) from the pre-industrial runs with the two mechanisms are plotted in Fig. 4. The first set of 10-year simulations have been carried out by not prescribing any fraction of SO$_2$ emission as direct sulphate particles; and for the other set, 5% of emission as primary sulphate particles going directly into the accumulation mode. Essentially, the accumulation mode particles are regarded as CCNs in the model, which turn into cloud droplets. The

Fig. 4 Annual averages: zonal distribution of preindustrial cloud droplet number concentration (droplets/cm^3)
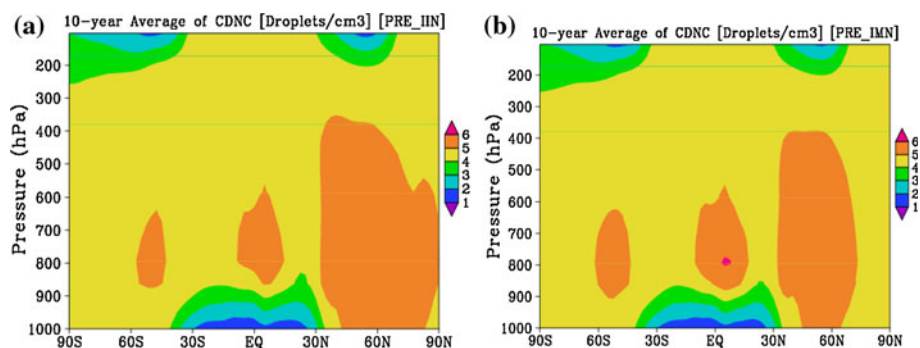

Fig. 5 Annual averages: zonal distribution of cloud droplet number concentration (droplets/cm^3)
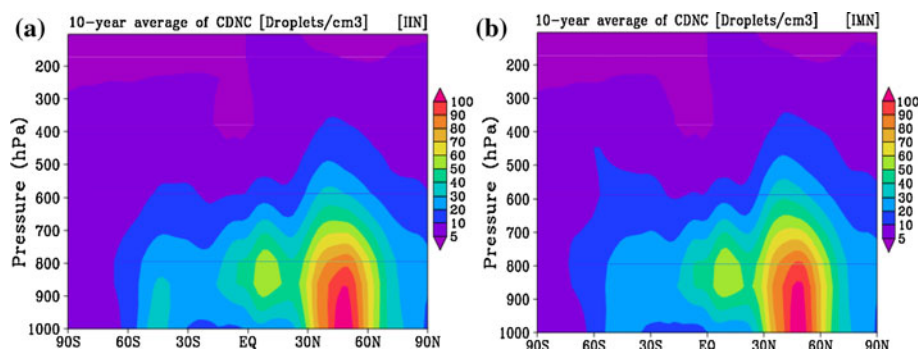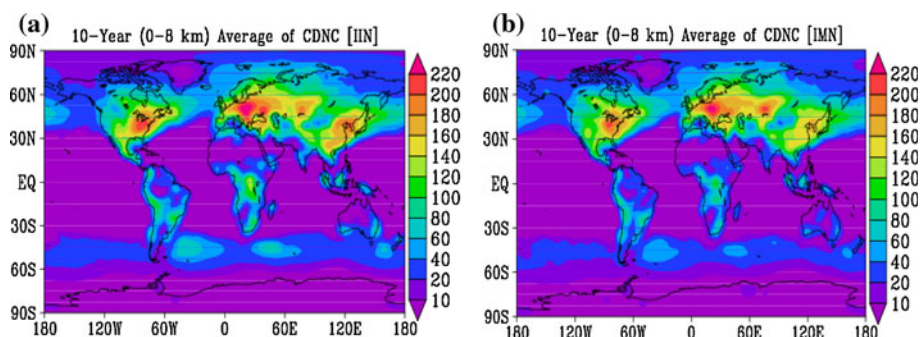

Fig. 6 Annual averages: horizontal distribution of cloud droplet number concentration (droplets/cm^3)

CDNCs are thus calculated from accumulation mode number concentration in the model using the expression for N_d given by Eq. 6. The zonal (Fig. 5) and horizontal (Fig. 6) distributions of annual averages of CDNCs from 10-year model runs with IIN and IMN nucleation mechanisms, show only minor differences while the nucleation rate in the IMN is much larger than that in the IIN. Why are then the differences in CDNCs small when the nucleation rates in the two mechanisms differ by an order of magnitude? The possible explanation could be that the accumulation mode particles form from particle growth due to condensation of H_2SO_4 vapour on existing particles, intra- and inter-modal particle coagulation mechanisms in the model. The H_2SO_4 vapour first condenses onto existing population of particles, and remaining amount of H_2SO_4 vapour, if any, is utilized in new particle formation. This paradigm is the key rate limiting process of new particle formation in the aerosol module wherein the rate of formation ($J_{3.5}$) of particles with 3.5-nm diameter is calculated using the Kerminen and Kulmala (2002) formulation from J_{IIN} and J_{IMN} which produce particles of diameters within an interval around 1 nm. From 3.5 nm diameter particles, the aerosol module predicts particle mass and number concentration in the two modes, viz., Aitken and accumulation modes. From particle number concentration in the accumulation mode, CDNC is calculated using formula (6) of Jones et al. (1994) in the model. Thus, in this sequence of computations, the intermediate differences in the calculations with IIN and IMN would continue to diminish at each stage of computation up to the final calculation of CDNC. This is why the differences in CDNCs simulated with IMN and IIN mechanisms would be small, even though their nucleation rates differ by an order in magnitude.

The simulated annual mean CDNC compares fairly well with the corresponding field derived from MODIS data (figure not shown here) by Quaas et al. (2006). Hence, the parameterization of Jones et al. (1994) for

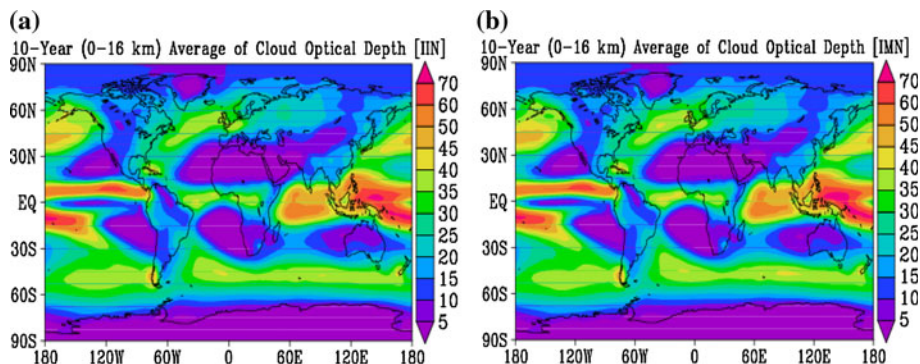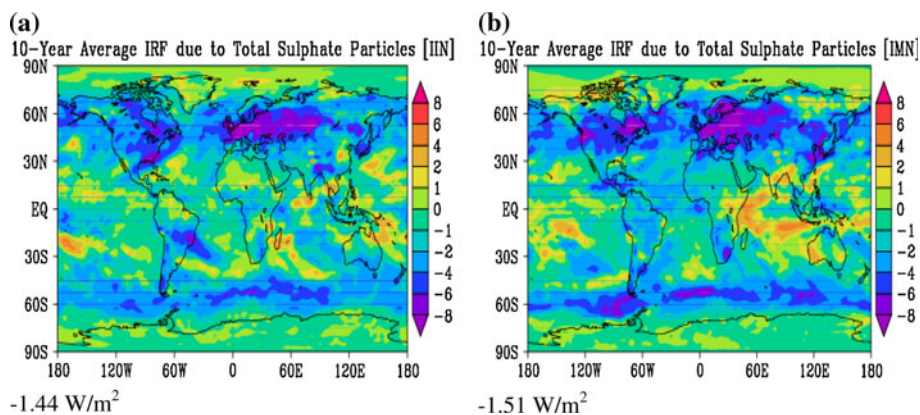**Fig. 7** Annual averages: horizontal distribution of cloud optical depth

Fig. 8 The 10-year average IRF (W/m²) without primary sulphate particles


-1.44 W/m²

-1.51 W/m²

CDNC computations (Eq. 6) is very successful in LMDZ. Mass transfer from Aitken to accumulation mode happens through various aerosol processes (intramodal, intermodal and condensation), and intermodal mass transfer would be more efficient in simulations with the IMN mechanism in the initial couple of years of simulations but as simulations extend further, the two mechanisms apparently produce similar horizontal distributions. It may also be confirmed with cloud optical depth fields shown in Fig. 7. The indirect radiative forcing, a derived quantity that depends on CDNC, has been calculated using Eqs. 11 and 12. The average indirect radiative forcing for sulphate particles is now discussed to bring out important differences in the response of the model that are induced by IIN and IMN mechanisms. The computation of indirect radiative forcing (Eq. 11) requires the computation of cloud radiative forcing (Eq. 12 with present-day and pre-industrial emission scenarios. Since indirect radiative forcing is defined as the difference in the CRF simulated for these two scenarios, therefore the model bias, if any, produced in the simulations will be eliminated. The indirect radiative forcing field should therefore present the true differences that are produced in the IIN and IMN runs. Wang and Penner (2009) have also calculated indirect radiative forcing due to particle nucleation using NCAR-CAM3 model, and they emphasized that aerosol indirect effects largely depend on changes in primary particles and SO_2 emission scenarios of preindustrial and present day. Therefore, emissions of primary particles are considered in the sensitivity runs to determine their impact on indirect radiative forcing. The 9-year averaged indirect radiative forcing fields from model simulations with no primary emitted sulphate particles have been presented in Fig. 8. Also, Table 1 summarizes results from 10-year runs with IIN and IMN where SO_2 emissions are prescribed at the preindustrial and present-day levels.

In these simulations, the cloud droplet concentration and the cloud radiative forcing are highly underestimated. The global annual averages of simulated CDNCs in the model are 20–21 droplets/cm³ (Table 1) while the formula (6) permits 375 droplets/cm³. Also, the global annual mean average of simulated shortwave cloud radiative forcing is −35 W/m² (Table 1); thus, in comparison to the observed CRF of −50 W/m², the simulated CRF is highly underestimated. The underestimation of cloud radiative forcing might be because only sulphate aerosols are present in this study. If primary emissions (e.g. dust, sea salt, carbonaceous aerosols) are included then clouds will be more reflective. Since indirect radiative forcing is calculated as the difference of CRF in the anthropogenic case and that of the preindustrial case, the indirect radiative forcing would

Table 1 10-year simulations with no primary particle emissions

Global mean value	IIN		IMN	
	Preindustrial	Anthropogenic	Preindustrial	Anthropogenic
CDNC (droplets/cm^3)	~4.54	~19.71	~4.56	~20.23
Cloud optical depth	~23.89	~23.897	~23.90	~23.956
Shortwave cloud forcing (W/m^2)	~ −34.78	~ −36.20	~ −34.84	−36.38

Fig. 9 The 10-year average IRF (W/m^2) with 5% direct sulphate particle emission
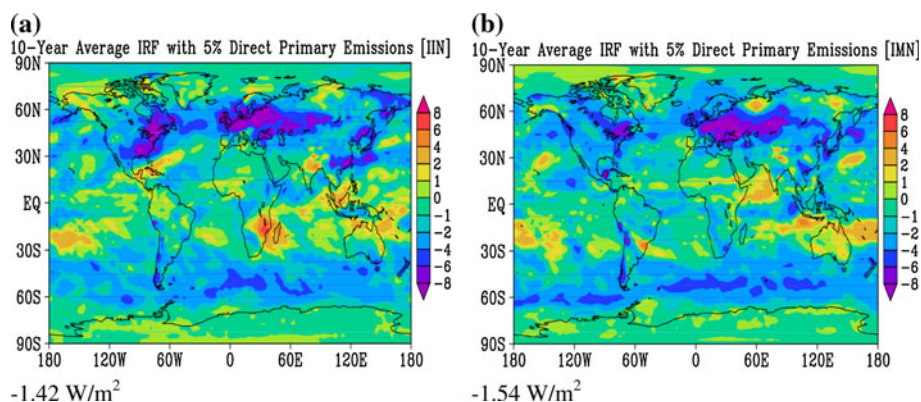
The cooling and warming associated with the indirect forcing (Fig. 8) from the 10-year runs is highly variable over the globe, but one may notice two prominent cooling zones in annual average indirect radiative forcing fields around 60°S in the 30–60°N latitudinal belt. The key warming areas over India, Indian Ocean and Western Australia are simulated in the IMN run (Fig. 8b). Radiative warming is generally simulated by both mechanisms in the tropics as seen in Fig. 8a, b, but prominent differences in warming are noticeable only over the Indian Ocean. Strong cooling over North America and Europe extending towards China may also be noted in the two simulations. In Table 1, one may also note a key difference in the simulated response: the annual mean global indirect radiative forcing calculated in this study from 10-year runs are −1.42 W/m^2 (IIN) and −1.54 W/m^2 (IMN). The differences in the response of the model in indirect radiative forcing (Fig. 8) are pronounced in the Arctic Region (Alaska and from Arctic Ocean to Baffin Bay) and the Indian Ocean. In these regions, model simulates relatively stronger positive indirect radiative forcing (warming) with the IMN.

Since the primary emissions of aerosol particles are an important source of the atmospheric aerosol particles (e.g., primary emissions of dust, sea salt, and carbonaceous aerosols), including primary aerosol particles in the model simulations are more realistic than not including them. Therefore, a fixed 5% sulphur mass from combustion sources is directly emitted as primary sulphate particles.

Because there is no other primary aerosol particles treated in the current model, the 5% emission of primary sulphate particles can act as a "proxy" for other primary aerosol particles. In the 10-year sensitivity runs with IIN and IMN mechanisms, direct emission of 5% sulphur mass from sources as grown up particles go to the accumulation mode. The annual averages of indirect radiative forcing from these simulations are presented in Fig. 9 and a significant impact of primary particles may be noted when these results are compared with those presented in Fig. 8. In the sensitivity runs, the model response with these two nucleation mechanisms is almost similar (Fig. 9) in the Arctic region and the warming over the Indian Ocean has also reduced for the IMN case. However, stronger warming is simulated over the Madagascar region in the IIN case and over the Arabian Sea in the IMN case.

The results of the sensitivity runs have been summarized in Table 2. A comparison of values of parameters in Tables 1 and 2 shows that CDNC and cloud radiative forcing have increased with the primary emitted sulphate particles in the simulations. The direct 5% emission of primary sulphate particles changes the indirect radiative forcing from −1.42 to −1.44 W/m^2 for IIN case, and from −1.54 to −1.55 W/m^2 for the IMN case. Thus, owing to greater nucleation rates, IMN mechanisms produces greater cooling than the IIN mechanisms in the backdrop that both mechanisms produce almost identical distribution of CDNC in their pre-industrial runs. These estimate very much fall in the range of indirect radiative forcing (−0.5 to −2.03 W/m^2) that has been reported in the literature (e.g.

Table 2 10-year simulations with 5% direct sulphate particle emissions

Global mean value	IIN		IMN	
	Preindustrial	Anthropogenic	Preindustrial	Anthropogenic
CDNC (droplets/cm^3)	~ 4.64	~ 19.87	~ 4.65	~ 20.95
Cloud optical depth	~ 23.89	~ 23.92	~ 23.92	~ 23.97
Shortwave cloud forcing (W/m^2)	~ -34.80	~ -36.24	~ -34.85	~ -36.40

Boucher and Lohmann 1995; Jones and Slingo 1996; Wang et al. 2009). While evaluating the response of several nucleation (except ion-promoted nucleation) mechanisms on aerosol indirect forcing, Wang and Penner (2009) have emphasized that the inclusion of primary particles increases the anthropogenic fraction of CCN concentration and the indirect radiative forcing from simulations with binary homogeneous nucleation mechanism and its variants, and empirical parameterization of boundary layer nucleation, but not with ion-promoted nucleation mechanisms. This study may therefore be considered as another contribution in this direction.

5 Conclusions

The response of two different nucleation mechanisms (IIN and IMN) has been examined in an atmospheric global model with interactive chemistry and aerosol dynamics. Both IIN and IMN mechanisms assume new particle formation from nucleation of sulphuric acid vapours on charged ions produced in the atmosphere by galactic cosmic radiation. The numerical simulations indicate that ion-mediated nucleation (IMN) generally gives higher nucleation rates in the tropospheric region in comparison to the ion-induced nucleation (IIN) in the common range of input variables. This result is consistent with the results of a recent study by Yu et al. (2010). This study also shows that, despite an order of difference in nucleation rates of IIN and IMN mechanisms, the patterns of cloud droplet number concentration and cloud optical depth resemble very closely both in the pre-industrial and anthropogenic runs. This is indeed a significant result from these simulations because both IIN and IMN mechanisms have large differences in their methodology and parameterizations, but produce almost similar response in the indirect radiative forcing. This is achieved by calculating the apparent nucleation rate of 3.5-nm particles using the Kerminen and Kulmala (2002) parameterization. Thus, aerosol processes, and the parameterizations play a key role in producing the net response of the model. Our results show that the response of these two nucleation mechanisms is better seen in the indirect radiative forcing as simulated by the model.

However, the CDNC and cloud radiative forcing are highly underestimated in the model simulations because only sulphate aerosols have been considered here.

Since the primary emissions of aerosol particles are an important source of the atmospheric aerosol particles (e.g., primary emissions of dust, sea salt, and carbonaceous aerosols), including primary aerosol particles in the model simulations are more realistic than not including them. Therefore, primary sulphate particles have been added in the model to act as a "proxy" for other primary aerosol particles. In the 10-year sensitivity runs with IIN and IMN mechanisms, the model response is almost similar; but stronger warming is simulated over the Madagascar region in the IIN case and over the Arabian Sea in the IMN case. However, it is important to mention that this conclusion solely lies on the formulation of computing CDNC from the accumulation mode particle concentration (Jones et al. (1994)), hence the results of this study could be sensitive to the parameterizations of CDNC. One key limitation of this study is related to coarse resolution model simulations, whereas for cloud microphysics and nucleation, it would be desirable to use a very high-resolution model. Therefore, the conclusions of this study should be viewed with these limitations of the simulations from resolution point of view as well. Thus, an important finding of this study is that response of IIN and IMN mechanisms in the indirect radiative forcing are nearly similar, except the Indian Ocean region, when primary emitted sulphate particles are included in numerical simulations. However, owing to higher nucleation rate, the IMN mechanism produces stronger cooling with the inclusion of primary particles in comparison to the IIN case. Since indirect radiative forcing is calculated as the difference of CRF in the anthropogenic case and that of the preindustrial case, the indirect radiative forcing estimates of this study would not be too underestimated and would fall well within the realistic range of indirect radiative forcing.

References

Binkowski FS, Roselle SJ (2003) Models-3 community multiscale air quality (CMAQ) model aerosol component: 1. Model description. J Geophys Res 108(D6):4183. doi:10.1029/2001JD001409

Binkowski FS, Shankar U (1995) The regional particulate matter model: 1. Model description and preliminary results. J Geophys Res 100:26191–26209

Boucher O, Anderson TL (1995) General circulation model assessment of the sensitivity of direct climate forcing by anthropogenic sulphate aerosols to aerosol size and chemistry. J Geophys Res 100:26117–26134

Boucher O, Lohmann U (1995) The sulphate-CCN-cloud albedo effect: a sensitivity study with two general circulation models. Tellus 47B:281–300

Chang L-S, Stephen ES, Robert M, Ernie RL (2009) Sensitivity of aerosol properties to new particle formation mechanism and to primary emissions in a continental-scale chemical transport model. J Geophys Res 114:D07203. doi:10.1029/2008JD011019

Clarke AD, Davis D, Kapustin VN (1998) Particle nucleation in the tropical boundary layer and its coupling to marine sulphur sources. Science 282:89–92

Feingold G, Koren I, Wang H, Xue H, Brewer WA (2010) Precipitation-generated oscillations in open cellular cloud fields. Nature 466:849–852. doi:10.1038/nature09314

Foley KM, Roselle SJ, Appel KW, Bhave PV, Pleim JE, Otte TL, Mathur R, Sarwar G, Young JO, Gilliam CG, Nolte CG, Kelly JT, Gilliland AB, Bash JO (2010) Incremental testing of the Community Multiscale Air Quality (CMAQ) modeling system version 4.7. Geosci Model Dev 3:205–226

Fouquart Y, Bonnel B (1980) Computations of solar heating of the earth's atmosphere: a new parameterization. Contrib Atmos Phys 53:35–62

Harrington YD, Kreidenweis SM (1998a) Simulations of sulphate aerosol dynamics–I. Model description. Atmos Environ 32(10):1691–1700

Harrington YD, Kreidenweis SM (1998b) Simulations of sulphate aerosol dynamics–Part II. Model intercomparison. Atmos Environ 32(10):1701–1709

Herald CL, Park DJ, Russell RJ, Huebert BJ, Seinfeld JH, Liao J, Weber RJ (2005) A large organic aerosol source in the free troposphere missing from current models. Geophys Res Lett 32:L18809. doi:10.1029/2005GL023831

Jones A, Slingo A (1996) Predicting cloud-droplet effective radius and indirect sulphate aerosol forcing using a general circulation model. Quart J Roy Meteor Soc 122:1573–1595

Jones A, Roberts DL, Slingo A (1994) A climate model study of indirect radiative forcing by anthropogenic sulphate aerosols. Nature 370:450–543

Kerminen V-M, Kulmala M (2002) Analytical formulae connecting the "real" and the "apparent" nucleation rate and the nuclei number concentration for atmospheric nucleation events. Aerosol Sci 33:609–622

Kulmala M, Laaksonen A, Pirjola L (1998) Parameterizations for sulphuric acid/water nucleation rates. J Geophys Res 103(D7):8301–8307

Laaksonen A, Hameed A, Joutsensaari J, Hiltunen L, Cavalli F, Junkermann W, Asmi A, Fuzzi S, Facchini MC (2005) Cloud condensation nucleus production from nucleation events at a highly polluted region. Geophys Res Lett 32:L06812. doi:10.1029/2004GL02292

Lee S–H, Reeves JM, Wilson JC, Hunton DE, Viggiano AA, Miller TM, Ballenthin JO, Lait LR (2003) Particle formation by ion nucleation in the upper troposphere and lower stratosphere. Science 301:1886–1889

Lovejoy ER, Curtius J, Froyd KD (2004) Atmospheric ion-induced nucleation of sulphuric acid and water. J Geophys Res 109:D08204. doi:10.1029/2003JD004460

Lucas DD, Akimoto H (2006) Evaluating aerosol nucleation parameterization in a global atmospheric model. Geophys Res Lett 33:L10808. doi:10.1029/2006GL025672

Makkonen R, Asmi A, Korhonen H, Kokkola H, Järvenoja S, Räisänen P, Lehtinen KEJ, Laaksonen A, Kerminen V-M, Järvinen H, Lohmann U, Bennartz R, Feichter J, Kumala M (2009) Sensitivity of aerosol concentrations and cloud properties to nucleation and secondary organic distribution in ECHAM5–HAM global circulation model. Atmos Chem Phys 9:1747–1766

Martin GM, Johnson DW, Spice A (1994) The measurement and parametrisation of effective radius of droplets in warm stratocumulus clouds. J Atmos Sci 51:1823–1842

Mebust MR, Eder BK, Binkowski FS, Roselle SJ (2003) Models-3 Community Multiscale Air Quality (CMAQ) model aerosol component, 2, Model evaluation. J Geophys Res 108(D6):4184. doi:10.1029/2001JD001410

Metzger A, Verheggenn B, Dommen J, Duplissy J, Prevot ASH, Weingartner E, Riipinen I, Kulmala M, Sparacklen DV, Carslaw KS, Baltensperger U (2010) Evidence for the role of organics in aerosol particle formation under atmospheric conditions. PNAS 107(15):6646–6651

Modgil MS, Kumar S, Tripathi SN, Lovejoy ER (2005) A parameterization of ion-induced nucleation of sulphuric acid and water for atmospheric conditions. J Geophys Res 110:D19205. doi:10.1029/2004JD005475

Morcrette JJ (1999) Radiation and cloud radiative properties in the European centre for medium range weather forecasts forecasting system. J Geophys Res 96:9121–9132

Nadykto A, Yu F (2003) Uptake of neutral polar vapour molecules by charged particles: Enhancement due to dipole-charge interaction. J Geophy Res 108(D23):4717. doi:10.1029/2003JD003664

Nair PVN, Vohra KG (1975) Growth of aqueous sulphuric acid droplets as a function of relative humidity. J Aerosol Sci 6:265–271

Pierce JR, Adams PJ (2009) Uncertainty in global CCN concentrations from uncertain aerosol nucleation and primary emission rates. Atmos Chem Phys 9:1339–1356

Pirjola L, O'Dowd CD, Kulmala M (2002) A model prediction of the yield of cloud condensation nuclei from coastal nucleation events. J Geophys Res 107:8098. doi:10.1029/2000JD000213

Quaas J, Boucher O, Lohmann U (2006) Constraining the total aerosol indirect effect in the lmdz and echam4 gcms using modis satellite data. Atmos Chem Phys 6:947–955. http://www.atmos-chem-phys.net/6/947/2006/

Sadourny R, Laval K (1984) January and July performances of LMD general circulation model. In: Berger A (ed) New perspectives in climate modelling. Elsevier, New York, pp 173–198

Spracklen DV, Carslaw KS, Kulmala M, Kerminen V-M, Mann GW, Sihto S-L (2006) The contribution of boundary layer nucleation events to total particle concentrations on regional and global scales. Atmos Chem Phys 6:5631–5648

Spracklen DV, Carslaw KS, Kulmala M, Kerminen V-M, Sihto S-L, Riipinen l, Merikanto J, Mann GW, Chipperfield MP, Wiedensohler A, Birmilli W, Lihavainen H (2008) Contribution of particle formation to global cloud condensation nuclei

concentrations. Geophys Res Lett 35:L06808. doi:10.1029/2007GL033038

Tang IN, Munkelwitz HR (1994) Water activities, densities, and refractive indices of aqueous sulphates and sodium nitrate droplets of atmospheric importance. J Geophys Res 99:18801–18808

Twomey SA (1959) The nuclei of natural cloud formation. Part II: The supersaturation in natural clouds and the variation of cloud droplet concentrations. Geofisica Pura e Applicata 43:227–242

Twomey SA (1977) Atmospheric aerosols, developments in atmospheric sciences. Elsevier Scientific publishing company, New York, p 7

Verma S, Boucher O, Upadhyaya HC, Sharma OP (2006) Sulphate aerosol forcing: an estimate using a three-dimensional interactive chemistry scheme. Atmos Environ 40:7953–7962. doi:10.1016/j.atmosenv.2006.07.010

Verma S, Boucher O, Reddy MS, Upadhyaya HC, Le Van P, Binkowski FS, Sharma OP (2007) Modeling and analysis of aerosol processes in an interactive chemistry general circulation model. J Geophys Res 112:D03207. doi:10.1029/2005JD006077

Wang M, Penner JE (2009) Aerosol indirect forcing in a global model with particle nucleation. Atmos Chem Phys 9:239–260

Wang M, Penner JE, Liu X (2009) The coupled IMPACT aerosol and NCAR CAM3 model: Evaluation of predicted aerosol number and size distribution. J Geophys Res 114:D06302. doi:10.1029/2008JD010459

Weber RJ, Marti IJ, McMurray PH, Eisele FL, Tanner DJ, Jefferson A (1996) Measured atmospheric new particle formation rates: implications for nucleation mechanism. Chem Eng Commun 151:53–64

Yu F (2005) Modified Kelvin-Thomson equation considering iondipole interaction: Comparison with observed ion-clustering enthalpies and entropies. J Chem Phys 122:084503. doi:10.1063/1.1845395

Yu F (2006) From molecular clusters to nanoparticles: second-generation ion-mediated nucleation model. Atmos Chem Phys 6:5193–5211

Yu F (2007) An improved quasi-unary nucleation model for binary H2SO4–H2O homogeneous nucleation. J Chem Phys 127:054301. doi:10.1063/1.2752171

Yu F (2010) Ion-mediated nucleation in the atmosphere: Key controlling parameters, implications, and look-up table. J Geophy Res 115:D03206. doi:10.1029/2009JD012630

Yu F, Luo G (2009) Simulation of particle size distribution with a global aerosol model: Contribution of nucleation to aerosol and CCN number concentrations. Atmos Chem Phys 9:7691–7710

Yu F, Turco RP (2000) Ultrafine aerosol formation via ion-mediated nucleation. Geophys Res Lett 27:883–886

Yu F, Turco RP (2001) From molecular clusters to nanoparticles: role of ambient ionization in tropospheric aerosol formation. J Geophys Res 105(D5):4797–4814

Yu F, Wang Z, Luo G, Turco R (2008) Ion-mediate nucleation as an important global source of tropospheric aerosols. Atmos Chem Phys 8:2537–2554

Yu F, Luo G, Bates TS, Anderson B, Clarke A, Kapustin V, Yantosca RM, Wang Y, Wu S (2010) Spatial distributions of particle number concentrations in the global troposphere: Simulations, observations, and implications for nucleation mechanisms. J Geophys Res 115:D17205. doi:10.1029/2009JD013473